University of Baghdad
College of Engineering
JE
JOURNAL OF ENGINEERING

Journal of Engineering

journal homepage: www.joe.uobaghdad.edu.iq

Volume 29 Number 6 June 2023

On the Laser Micro Cutting: Experimentation and Mathematical Modeling based on RSM-CCD

Sura Sabah Hassan[1,*], Bassim Shaheen Bachy[2]
Department of Mechanical Engineering, College of Engineering, University of Baghdad, Baghdad- Iraq
sura.hassan2003m@coeng.uobaghdad.edu.iq[1], b.bachy0903@coeng.uobaghdad.edu.iq[2]

ABSTRACT

The laser micro-cutting process is the most widely applied machining process, which can be applied to practically all metallic and non-metallic materials. While this had challenges in cutting quality criteria such as geometrical precision, surface quality, and numerous others. This article investigates the laser micro-cutting of PEEK composite material using nano-fiber laser due to the significant importance and efficiency of laser in various manufacturing processes. Design of Experiential tool based on Response Surface Methodology **(DoE-RSM)** Central Composite Design **(CCD)** used to generate the statistical model. This method was employed to analyze the influence of parameters, including laser speed, laser power, laser frequency, and the number of passes on the cutting characteristics -and geometrical. Cutting-geometry requirements are significant quality features since they are one of the metrics for the geometrical precision of micro-cutting process. It was concluded that higher laser power, slower speed, and more pass number result in a low kerf taper; these parameters significantly impact the other cutting characteristics and groove geometry. Whereas the frequency has a lower impact on the cutting geometry. Finally, the experiments show that the maximum cutting depth was 2000μm, with minimum upper width of 305.56 μm and a minimum angle of 2.8906^{o}.

Keywords: PEEK material, laser micro-cutting process, fiber laser.

*Corresponding author
Peer review under the responsibility of University of Baghdad.
https://doi.org/10.31026/j.eng.2023.06.08

Article received: 02/01/2023
Article accepted: 06/02/2023
Article published: 01/06/2023

القطع الدقيق باستخدام الليزر: دراسة عملية والنمذجة باستخدام الRSM-CCD

سرى صباح حسن[1,*] ,باسم شاهين بجاي[2]
قسم الهندسة الميكانيكية, كلية الهندسة, جامعة بغداد

الخلاصة

تعتبر عملية القطع بالليزر واحدة من أكثر عمليات المعالجة شيوعًا لكفاءتها في تقطيع أصعب المواد المعدنية والغير معدنية والمركبة منها أيضا. وعلى الرغم من ذلك الا نها تعاني من الكثير من المشاكل الي تخص جودة السطح ودقة الابعاد اضافة لأهمية هذه العملية فقد تم التوجه لطرق التحليل الحديثة مثل تصميم التجارب ومنهجية الاستجابة السطحية (DoE-RSM) والتصميم المركب المركزي (CCD) المستخدم لإنشاء النموذج الإحصائي حيث استخدامه هذه الطريقة لتحليل تأثير المتغيرات نظرا لقدرتها وكفاءتها الجيدة في اجراء عملية نمذجة في مختلف العمليات الصناعية والطبية الأخرى. يهدف هذا البحث في اختبار النانو ليزر الألياف ومركب PEEK. ودراسة العلاقة المعقدة للمتغيرات الاتية سرعة القطع، وقوة الليزر، وتردد الليزر وعدد التمريرات على الخصائص الهندسية للقطع وابعاده. وتعتبر متطلبات القطع من سمات الجودة الهامة لأنها أحد مقاييس الدقة الهندسية للتجاويف وقد استنتج من خلال الجانب العملي الحالي أن كل من القوة والسرعة وعدد التمريرات لها تأثير كبير على الخصائص الهندسية للشق وتؤدي طاقة الليزر العالية جدا، والسرعة القليلة، والمزيد من التمريرات إلى انخفاض في زاوية الشق. وهذه المتغيرات كانت الأكثر فعالية في تغيير وتحسين ابعاد وشكل الشق. في الختام أظهرت النتائج العملية ان (μ 305.56m) هي اقل قيمة سجلت في قطر علوي وبزاوية (2.8906^{o}) بقطع كامل 2000µm

الكلمات الرئيسية: مادة PEEK، عملية قطع ميكروية بالليزر، الليزر الليفي.

1. INTRODUCTION

Since the 1970S, laser beams have been used in numerous manufacturing processes. In practically all categories of materials, such as metals, non-metals, ceramics, and composites, laser beam machining, one of the non-conventional cutting processes, is widely utilized to produce complicated shapes and various geometries with thin kerf. Due to the growing need for high product quality, productivity, and specialized requirements concerning geometric accuracy, micro-size, and shape, Modern industrial companies increasingly rely on non-conventional machining technologies **(Madić et al., 2022).** The terminology "kerf" describes the slot created by material dissolution, and Kerf Width "KW" refers to the amount of extra material removed (width of the cut slot). As a result, the laser's slot is known as a kerf, and its width is known as the KW **(Mushtaq et al., 2020).** The illustration of KW is shown in **Fig. 1.**

In previous years, the main criteria and purpose of the research were oriented on investigating the resulting kerf geometrical characteristics of the cutting edge, such as kerf perpendicularity **(Varsi and Shaikh, 2019),** Taper angle and width **(Dixit et al., 2019; Son and Lee, 2020; Girdu et al., 2021)**, Deviation in kerf **(Tamilarasan and Rajamani, 2017; Mishra et al., 2020),** Geometric accuracy **(Ninikas et al., 2021)**, and dross formation **(Spena, 2017)**. The investigation of cut surfaces performance characteristics such as surface

striations and Micro hardness has attracted the attention of numerous researchers. The physical–chemical properties of the material in the cut surface layer **(Rodrigues et al., 2018**). Heat-affected-zone **(Sen et al., 2016; Patel and Bhavsar, 2020)**. This is a significant criteria in micro-cutting processes, since the quality of cutting, and the efficiency of the laser depend mostly on the selection of the primary process variables. A poor selection of these parameters results an inefficient processing and the formation of undesirable outcomes such as dross, heat-affected zones, and striations.

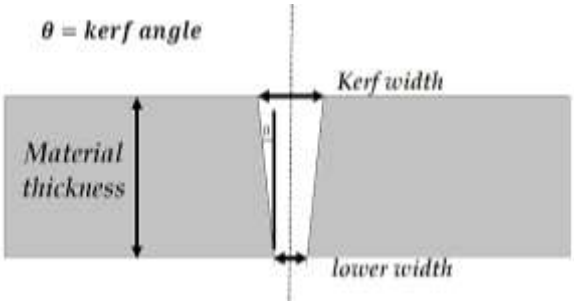

Figure 1. The cross-section profile.

(Pramanik et al. 2021) studied the effect of low-power fiber laser beam machining on cutting stainless steel AISI 316 L with 1 mm thickness (50 Watts). The cutting wedge angle has been looked at in terms of energy, duty cycle, pulse frequency, and scanning speed. They concluded that the kerf taper increases with the power of the laser beam energy. At the focus of the laser beam, where the power is high, the top surface of the work sample melts, releasing heat energy. As a result, it vaporizes instantly and creates a significant taper by removing a significant amount of material from the top surface during penetration. The laser beams at low intensity create a small taper. When the cutting wedge angle was 0.5°, the minimum kerf taper was 0.4642^{o}, the cutting speed was 0.60 mm/sec, the pulse frequency was 60 kHz, the duty cycle was 86%, and the working power was 46.2450 W. (**Wang et al., 2020)** created microchannels on the surface of stainless steel. They used scanning speed and frequency and many different factors to study the responses of the heat-affected zone (HAZ), the cutting width, depth of cut, and material removal rate (MRR). In this work, the process parameters have been optimized based on (RSM) method. The optimal processing settings are 10.4 J pulse energy, 15.8 kHz frequency, and 2.7 mm/s scanning speed.

(Varsi and Shaikh, 2019) used full-factorial design to examine the multiple passes on 8mm thick polymer material with a CO_2 laser. They studied the influences of laser cutting parameter such as laser power, cutting speed, and passes number on the cutting quality for kerf taper angle and said that at relatively high passes, the stand-off-distance increases, resulting in less energy transfer and greater kerf tapers. The minimal kerf taper value is 4° for 22.75W, 0.202 m/s, and five passes. As a result, to obtain the lowest kerf taper, a combination of a higher power, lower speed, and a greater number of passes should be chosen. **(Sen et al., 2016)** also, use fiber laser to investigate the influence of scan speed pulse frequency, average power, and number of passes with Poly-methyl-methacrylate (PMMA) on different process parameter settings that leads to different width and depth of the microchannels. Conclude that the effect of the number of passes leads to more uniformity of the microchannel profiles and significant improvement in the depth of the microchannels, with the increment of scan speed with different settings of average laser power leading to

reduce the width of microchannels due to the effect of sputtering and less material interaction time.

(Teixidor et al., 2014) investigated fiber laser experiments for cutting stainless steel 316L sheets. The influence of peak pulse power, pulse frequency, and cutting speed on cutting quality was explored for fixed gas type and gas pressure, and a mathematical model for dross dimensions was developed. The dross height and diameter were measured and compared to the experimental findings. Both dimensions rise as the pulse peak power increases. **(Spena, 2017)** showed an increase in laser power causes the top kerf to grow. Because more thermal energy is provided to the steel sheet blanks per unit of time, wider regions are melted, whereas low cutting speeds allow a greater overlapping of laser pulses. **(Genna et al., 2020)** investigated the effects of cutting speed with different laser parameters such as material type, gas pressure, workpiece thickness, and laser cutting kerf quality. They designed a systematic factorial design based on Design of Experiments (DoE) material to investigate the various control variables and provided suggestions for optimal cutting settings for St37-2 low-carbon steel, $AlMg_3$ aluminum alloy, and AISI 304 stainless steel. As a result, the top kerf width was mainly affected by the workpiece thickness, material type, and thickness, which strongly influenced the bottom kerf width. The gas pressure taper angle was mostly affected by the material type.

In this work, a polymer plate reinforced with fiberglass (composite material) is used to investigate the influence of laser micro-cutting parameters, including cutting speed (V) with a range of 10 to 50mm/s, laser power (P) between 20 to 40W, frequency (f) range of 50 to 70 kHz and number of passes have 1-9 per-passes on the characteristics of kerf geometry values including kerf width, depth, and taper angle. The experimental work employed the DoE tools based on (RSM-CCD) response surface methodology (RSM)-central composite design (CCD) design. A second-order mathematical model using multi-regression analysis that compares the kerf criteria and the process parameters is obtained. So, the variation of the geometry criteria with power, speed, frequency, and the number of passes can be predicted.

2. THE RSM MATHEMATICAL MODEL

RSM is a set of statistical and mathematical tools that can determine how the response and the relationship between the independent variables relate to each other. When the independent variables are used alone or together, RSM determines the performance of processes. This experimental method creates a mathematical model and examines the impacts of the independent variables. Response Surface Methodology comes from the mathematical model being seen as a graph **(Ba and Boyaci, 2007).**

Central Composite Design (CCD) is a response surface design that includes an axial or star point along with the three-level elements. The axial or star point, commonly indicated as (α), raises the number of levels to 5, allowing the experimental design to be more flexible. Its advantage over Box-Behnken is that it allows the experiment designer to understand what influence the variables had on response when the experimental designer goes over or below the selected factors. The generic quadratic equation was used to reference the independent parameters to the replies, which is given by **(Bachy, 2017)**.

$$\gamma = \beta_o + \sum_{i=1}^{k} \beta_i x_i + \sum_{i=1}^{k} \beta_{ii} x_i^2 + \sum_{i=1}^{k} \beta_{ij} x_i x_j + \varepsilon \quad (1)$$

where:

γ is the response.

β_o, β_i, β_{ii} and β_{ij} are constant, linear, quadratic, and interaction coefficients, respectively.

x_i and x_j represent independent variables (input parameters).

k is the number of input parameters.

ε is the residual error (μm).

Eqs. (1) to (4) are used to determine the three responses for groove geometric including (depth, upper width, and angle).

$$\sum_{i=1}^{k} \beta_i x_i = \beta_1 v + \beta_2 p + \beta_3 f + \beta_4 pno \quad (2)$$

$$\sum_{i=1}^{k} \beta_{ii} x_i^2 = \beta_{11} v^2 + \beta_{22} p^2 + \beta_{33} f^2 + \beta_{44} pno^2 \quad (3)$$

$$\sum_{i=1}^{k} \beta_{ij} x_i x_j = \beta_{12} v.p + \beta_{13} v.f + \beta_{14} v.pno + \beta_{23} p.f + \beta_{24} p.pno + \beta_{34} f.pno + \varepsilon \quad (4)$$

where:

p is the laser power (W).

v is the laser speed (mm/s).

f refers to the laser frequency (kHz).

pno is the laser passes numbers.

3. EXPERIMENTAL SETUP AND PROCEDURES

A series of experimental experiments were carried out to explore the influence of the input process factors on the laser micro-cutting geometric. A CAD/CAM software program, EzCad 2, has been used for parameter definition, input, and cutting CAD design. Practical experiments were performed using the machine specification of the details in **Table 1.**

Table 1. Machine specification

Specification	Description
Laser Type	Fiber laser
Wavelength	1064 nm
Max. Power	50 W
Max. Pulse Frequency	200 kHz
Plus Duration	20 ns
Beam Diameter	30 μm
Max. Speed	10000 mm/s

The material utilized in this work is a black (Vectra E840i) a thermoplastic composite plate of Polyether ether ketone (PEEK) reinforced with glass fiber. These materials are intended for manufacturing circuit boards, transportation, aerospace, building, and medical equipment.
The entire parameters investigated in this work are listed in **Table 2.** The variables: cutting laser speed, laser power, laser frequency, and passes number in the range of (10 to 50 mm/s), (20 to 40 W), (50 to70 kHz), and (1 to 9), respectively, are the input parameters for this work based on RSM central composite design (CCD) to the influence of the laser on the geometry of the applied material.

Table 2. Controllable Parameters and Levels

Controllable parameters	Units	Levels				
		-2	-1	0	1	2
Cutting Speed (V)	mm/sec	10	20	30	40	50
Working Power (P)	W	20	25	30	35	40
Pulse Frequency (f)	Hz	50	55	60	65	70
Pass Number (P.N)		1	3	5	7	9

The experimental RSM-CCD design includes 28 tests. The main advantage of using this technique is that it allows for properly examining each design element's influence on the quality indicator.
On samples, when the laser's focal length is always 8 cm, the incidence angle is always 0o. Therefore, the spot diameter is always 0.05 mm, and a vertical line with a length of 15 mm has been created. The test samples were cut into squares with a cross-section of 20 mm x 30 mm and a thickness of 2 mm. The geometrical response variables were measured using (the MEIJI microscope) video microscopy system. The responses of top width, depth, and angle were selected. Each measurement was repeated using Image j soft three times, and the average value was recorded as the ultimate result.

4. RESULTS AND DISCUSSION

4.1 Experimental Results

The experimental runs were determined using the RSM-CCD design matrix, and the kerf criteria readings were displayed in 28 experiments. **Table 3** illustrates the cut characteristics, including top width, depth dimensions, and taper angle, which have been measured. **Figs. 2 to 5** show the process parameters' effects on the PEEK material's cut profile. It can be seen that the cut depth improves as laser power and the number of passes increase or reduces with laser speed and frequency. As the laser power or the number of passes increases, the amount of heat input on the polymer's interface rises, and the volume of material removed from the material surface is increased too, as illustrated in **Figs. 2 and 3** allowing the cut depth of grow **(Bachy and Franke, 2015)**. Also, it can be noticed that the influence of the input variables on cut width has the same effect on depth.

Table 3. Experimental results.

	Parameters				Results		
TEST NO.	Actual setting parameters				Dimensions of microgroove.		
	Velocity (mm/sec)	Power (W)	Frequency (kHz)	Pass. No	Top (μm)	Depth (μm)	Angle (deg)
1	20	25	55	3	351.3	1459	5.317
2	40	25	55	3	305.56	934.5	7.1353
3	20	35	55	3	368.23	2000	4.183
4	40	35	55	3	320.2	1430.9	5.354
5	20	25	65	3	310.12	1200	8.561
6	40	25	65	3	308.45	1012.6	8.329
7	20	35	65	3	356.6	2000	3.7823
8	40	35	65	3	319.56	1524.5	3.8806
9	20	25	55	7	358.2	2000	3.746
10	40	25	55	7	354.2	1531.7	4.037
11	20	35	55	7	370.11	2000	3.8746
12	40	35	55	7	364.21	2000	4.8676
13	20	25	65	7	362.33	2000	6.3053
14	40	25	65	7	355	2000	3.9773
15	20	35	65	7	370.35	2000	3.6943
16	40	35	65	7	365.21	2000	3.6147
17	10	30	60	5	368.29	2000	4.5986
18	50	30	60	5	315.33	1480.5	4.688
19	30	20	60	5	309.5	1126.5	6.035
20	30	40	60	5	357	2000	2.8906
21	30	30	50	5	355.4	1552.5	3.4553
22	30	30	70	5	360.4	2000	3.6463
23	30	30	60	1	310.7	1390.4	8.4863
24	30	30	60	9	367.65	2000	5.8763
25	30	30	60	5	369.54	2000	3.3555
26	30	30	60	5	369.54	2000	3.3555
27	30	30	60	5	369.54	2000	3.3555
28	30	30	60	5	369.54	2000	3.3555

As the frequency of the laser increases in **Figs. 4a and b,** the kerf dimensions reduce lead from a decrease in the plus duration, which reduces the heat input onto the surface of the polymer, and the amount of material removed from this fig, the latte was less visible. The number of passes had the greatest influence on the taper angle. Given the slow speed, the laser has more time to stay in contact with the profile resulting in a more concentrated and high-depth penetration. Furthermore, at medium to high passes number 5-9 and laser power 30w laser speed 30mm/s and frequency 50 kHz, 70 kHz, there is no high effect of frequency on the width, depth, and angle of taper as shown in **Figs. 4c, d, and Fig. 5** show that decreasing the cutting speed improved the cut width due to the higher energy supplied.

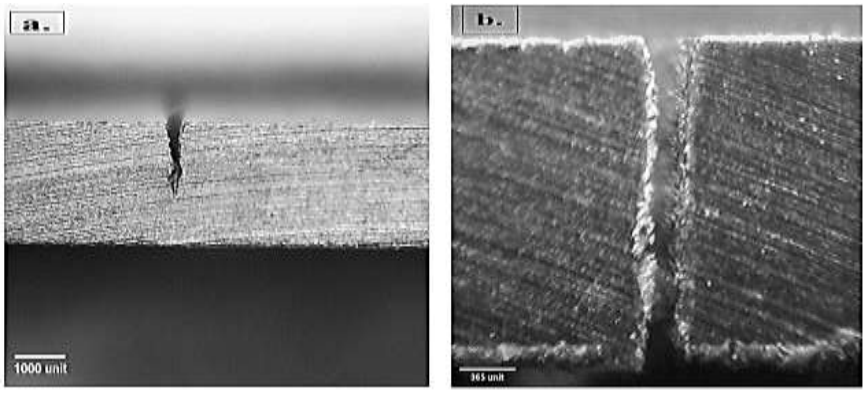

Figure 2. Topography images for the material at (a) 20 W, (b) 40W, with V=30 mm/s, f=60 kHz, and P.N =5.

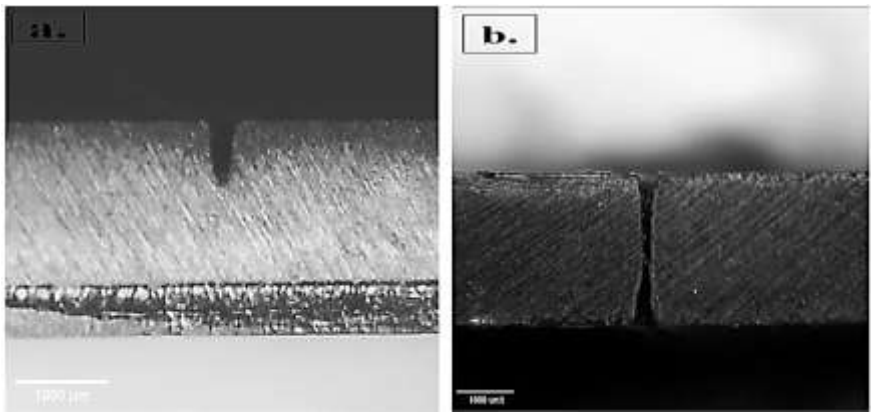

Figure 3. Topography images for the PEEK material show the effect of P.N on kerf geometrical (a) 1(b) 9 at P=30 W, V=30mm/s, f=60 kHz

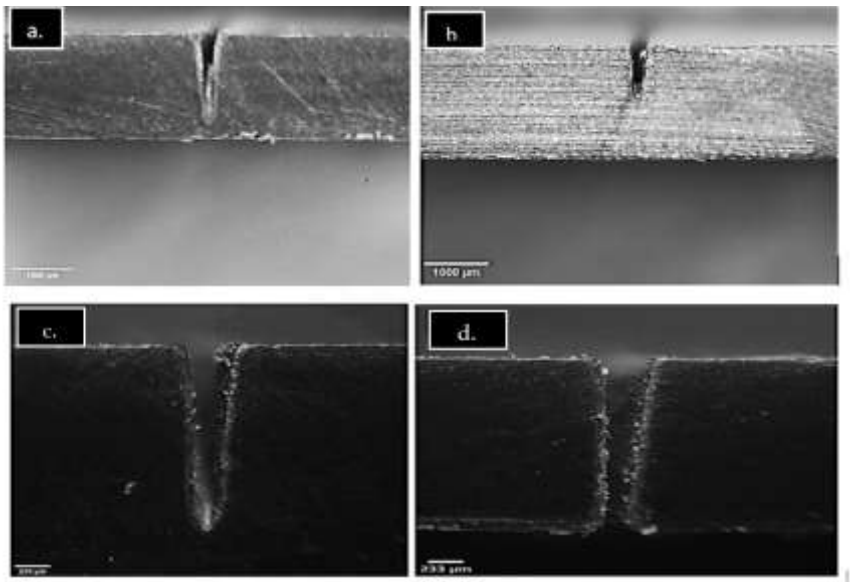

Figure 4. Topography images for the material at (a)55 kHz. (b)65 Hz, with P=25 W, V=20 mm/s and P.N =1, (c)50 kHz (d)70 kHz, with P=30 W, V=30 mm/s and P.N =5.

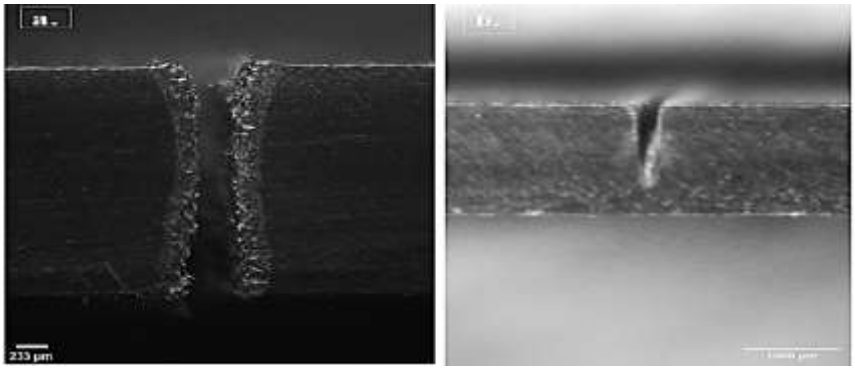

Figure 5. Topography images for the material at (a)10mm/s(b)50mm/s, with P=30W, f=60 kHz, and p.no =5.

4.2 Theoretical Results

ANOVA is a statistical technique for examining responses (output parameters) affected by various variables (input parameters). Each experiment involves modifying the input variables to establish the cause of variations in the predictor variables. The goal is to create a mathematical model with the minimum errors possible that illustrates a relationship between inputs and outputs (parameters and responses). Depending on the type of input, variable parameters might vary. The RSM technique was used to create the second-order mathematics equation. Eqs. (4) to (7) are used to calculate the three groove geometric responses (depth, width, and angle). The mathematical model's determination is presented below.

$$depth = -11666 - 67.8\,v + 381.0p + 239f + 333pno - 0.642\,v^2 - 4.34\,p^2 - 2.21\,f^2 - 20.03pno^2 + 0.170v.p + 1.124\,v.f + 4.03v.pno - 0.48p.f - 11.75p.pno + 3.48\,f.pno \quad (5)$$

$$top = 139 - 1.50\,v + 21.95p + 5.71f + 3.0\,pno - 0.0640v^2 - 0.3416p^2 - 0.0951f^2 - 1.765\,pno^2 - 0.0467v.p + 0.0656v.f + 0.3441v.pno + 0.0558\,p.f - 0.306\,p.pno + 0.355\,f.pno \quad (6)$$

$$angle = 117.1 + 0.281v + 0.254\,p + 0.804f - 3.757pno + 0.003356\,v^2 + 0.01162\,p^2 + 0.00250f^2 + 0.2425pno^2 + 0.00329\,v.p - 0.00852\,v.f - 0.01244\,v.pno - 0.02561\,p.f + 0.06330\,p.pno - 0.00936\,pno.f \quad (7)$$

The coefficient for each process variable represents the impact of all these variables on the final process response, as shown in the above modeling formulas. For instance, in the depth cut produced model, it can be seen that $\beta_2 > \beta_4 > \beta_3 > \beta_{14} > \beta_{34} > \beta_{13} > \beta_{12} > \beta_1 > \beta_{44} > \beta_{24} > \beta_{22} > \beta_{33} > \beta_{11} > \beta_{23}$. The fig below represents the mean effect for input variables.

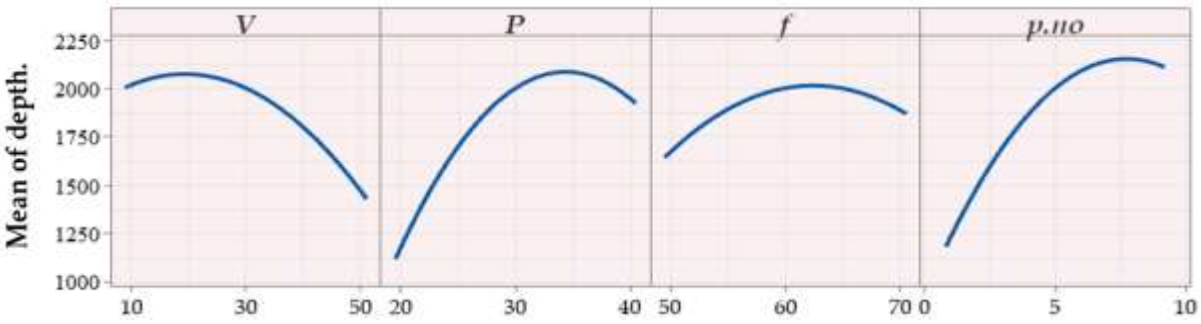

Figure 6. The interaction between the process parameters and its effect on depth cut.

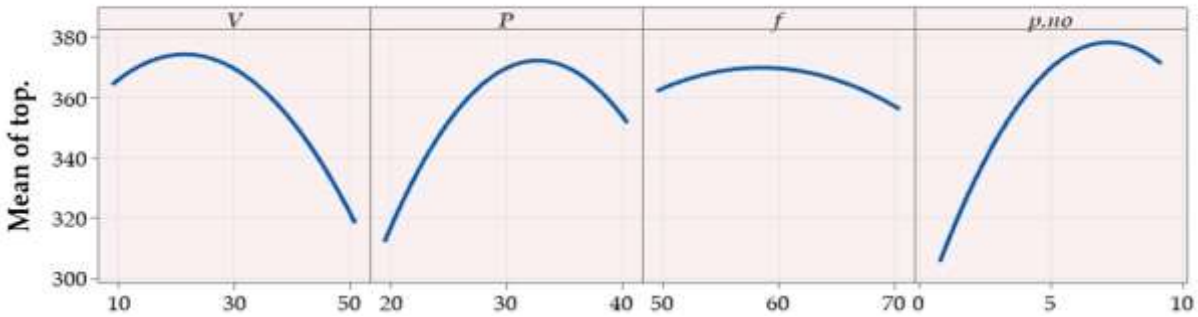

Figure 7. The interaction between the process parameters and its effect on the groove top.

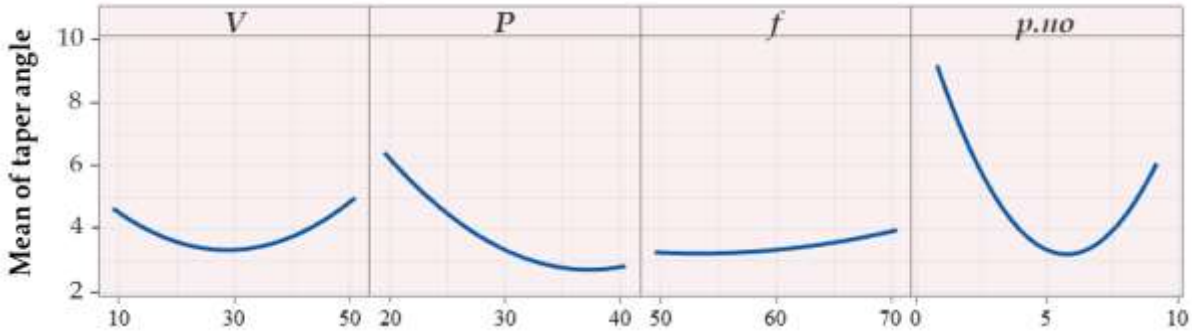

Figure 8. The interaction between the process parameters and its effect on taper angle.

Figs. 6 and 7 illustrate the main effects plot for depth and top Width. Laser velocity has different behavior observed. The laser's speed has an inverse influence. As it seems between 10 and 30 mm/s, the overlap (pluses per spot) and dose increase, which leads to the top width and depth of cut getting bigger, while at high speeds, the irradiation duration between the laser and the material was minimized. Moreover, it can be seen that the effect of laser micro-cutting parameters on the width is the same as on the groove depth

Due to the lower power supplied (30-40 W), the top width is decreased. Whereas it is clear that the laser power and the pass number have a positive influence, while the frequency has almost no influence on the mean of this response, as shown in **Fig. 4**. It can be noted when the laser frequency rise from 50kHz to 70 kHz, the kerf depth and top width remain constant.

Fig. 8 illustrates the mean effect plot for the angle of the taper. Lower speed and more power play an important role in improving the kerf angle. Because of the slow speed, the laser has more time to stay in contact with the profile, producing a low kerf taper. When laser power increases, the kerf angle taper decreases significantly. The laser beam's heat enters the surface most during the high-power setting. This results in a larger kerf width with a low taper angle, and when the 30 mm/s value is used, it is noticed that as the value of high-speed result angle of taper raised too. The rise in the angle of the taper with increasing speed is because the laser's heat concentration is reduced, resulting in less material evaporation, which causes it to be minimized. The depth and the kerf taper slowly grow.

The impact of the passes numbers is clearly shown in Fig. 8. As it is increased from 1 to 5, the taper decreases (improves), and at higher passes from 5 to 9, has changed in focus length, which results in a loss of energy transfer Passes number and laser power have the most influential factor for the three responses. In general, an increase in passes increases the depth, and top width consequence due to the more thermal energy and more material removal rate increase lends small kerf taper. Creating large kerf tapers will probably be related to the taper angle increasing as the top width changes more quickly than it varies at lower depths.

Table 4. ANOVA for the depth model.

Source	DF	Adj SS	Adj MS	F-Value	P-Value
Model	14	3309555	236397	15.30	0.000
Linear	4	2533620	633405	40.99	0.000
V	1	443945	443945	28.73	0.000
P	1	867937	867937	56.16	0.000
F	1	67788	67788	4.39	0.056
p.no	1	1153950	1153950	74.67	0.000
Square	4	377750	94438	6.11	0.005
V*V	1	99011	99011	6.41	0.025
P*P	1	282435	282435	18.28	0.001
f*f	1	73221	73221	4.74	0.049
p. no*p.no	1	153996	153996	9.96	0.008
2-Way Interaction	6	398185	66364	4.29	0.013
V*P	1	1157	1157	0.07	0.789
V*f	1	50562	50562	3.27	0.094
V*p.no	1	103785	103785	6.72	0.022
P*f	1	2334	2334	0.15	0.704
P*p.no	1	221018	221018	14.30	0.002
f*p.no	1	19328	19328	1.25	0.284
Error	13	200900	15454		
Lack-of-Fit	10	200900	20090		
Pure Error	3	0	0		
Total	27	3510455			
S=124.313,	R_sq(adj)=88.11%		Rsq(pred)=67.04%		Rsq=94.28%

Table 5. ANOVA for the top model.

Source	DF	Adj SS	Adj MS	F-Value	P-Value
Model	14	14894.8	1063.91	17.34	0.000
Linear	4	10791.4	2697.85	43.96	0.000
V	1	2833.4	2833.37	46.17	0.000
P	1	2096.5	2096.46	34.16	0.000
F	1	49.3	49.28	0.80	0.387
p.no	1	5812.3	5812.28	94.71	0.000
Square	4	2703.7	675.93	11.01	0.000
V*V	1	983.1	983.14	16.02	0.002
P*P	1	1750.5	1750.49	28.52	0.000
f*f	1	135.7	135.70	2.21	0.161
p. no*p.no	1	1195.9	1195.93	19.49	0.001
2-Way Interaction	6	1399.7	233.28	3.80	0.021
V*P	1	87.3	87.28	1.42	0.254
V*f	1	172.2	172.20	2.81	0.118
V*p.no	1	757.8	757.76	12.35	0.004
P*f	1	31.2	31.16	0.51	0.489
P*p.no	1	150.1	150.12	2.45	0.142
f*p.no	1	201.1	201.14	3.28	0.093
Error	13	797.8	61.37		
Lack-of-Fit	10	797.8	79.78		
Pure Error	3	0.0	0.00		
Total	27	15692.6			
S=7.83406, R_sq(adj)=89.44%, Rsq(pred)=70.72%, Rsq=94.92%					

The ANOVA analysis is presented in **Tables 4 to 6,** which exhibit the ANOVA outcomes for each response shown in the tables above where: P is the laser power, V is the laser speed, f refers to the laser frequency, and p.no is the laser passes numbers.

As shown in **Table 4.** depending on the p-value and f-value, it is clear that the effect of the number of passes, laser power, and velocity is more than that for the laser frequency. With the interactions of f, v*P, v*f, P*f, and f*pno, the statistical analysis indicated that all major effects were significant at a 95% confidence level for the depth model. The remaining adequacy indicators, R^2, adjusted R^2, and predicted R^2, are in an acceptable range and close to one, indicating that the model is adequate. The largest effect or significance (corresponding to the highest F-value) concerning depth kerf was attained by adjusting the number of passes, laser power, laser speed, and frequency.

Table 5. represents the ANOVA result for the top model, the factors f, f*f, V*P, V*f, P*p.no, f*p.no, with p-value more than 5%, the (adj)R^2 and R^2 are 89.44%, 94.92%, respectively. The pass number strongly influences the top, followed by laser speed and power.

The resulting angle model is given in **Table 6**. The insignificant factors are V, f, f*f, V*P, f*p.no, the R^2- (adj) R^2 and R^2 are 94.87% and 97.53%, respectively, and the most influences were laser power second the passes number.

Table 6. ANOVA for the angle model.

Source	DF	Adj SS	Adj MS	F-Value	P-Value
Model	14	72.6156	5.1868	36.66	0.000
Linear	4	31.2129	7.8032	55.15	0.000
V	1	0.1522	0.1522	1.08	0.319
P	1	17.4165	17.4165	123.09	0.000
f	1	0.6706	0.6706	4.74	0.049
p.no	1	12.9737	12.9737	91.69	0.000
Square	4	23.9659	5.9915	42.34	0.000
V*V	1	2.7025	2.7025	19.10	0.001
P*P	1	2.0246	2.0246	14.31	0.002
f*f	1	0.0936	0.0936	0.66	0.431
p. no*p.no	1	22.5847	22.5847	159.61	0.000
2-Way Interaction	6	17.4368	2.9061	20.54	0.000
V*P	1	0.4335	0.4335	3.06	0.104
V*f	1	2.9027	2.9027	20.51	0.001
V*p.no	1	0.9898	0.9898	7.00	0.020
P*f	1	6.5600	6.5600	46.36	0.000
P*p.no	1	6.4107	6.4107	45.31	0.000
f*p.no	1	0.1401	0.1401	0.99	0.338
Error	13	1.8394	0.1415		
Lack-of-Fit	10	1.8394	0.1839		
Pure Error	3	0.0000	0.0000		
Total	27	74.4550			
S=0.376158, R-sq=97.53%, R-sq(adj)= 94.87%, R-sq(pred)= 85.77%					

5. CONCLUSIONS

In this study, the influence of laser micro-cutting variables on cut dimensions and quality has been investigated. The process parameters are laser power, cutting speed, frequency and the number of laser passes, and cut quality. The kerf characteristics, including kerf width, depth, and taper angle, were evaluated using DoE based on RSM-CCD. The conclusions drawn could be summarized as follows:

1. The kerf characteristics, including depth, upper width, and angle, were strongly influenced by laser parameters and increased with the laser power and pass number or

when the laser speed and frequency were reduced. Furthermore, at medium-high 5-9 passes, the effect of the pass number and laser power on the cut profile and dimensions are always stronger than the effects of laser frequency and speed.

2. In a multi-pass condition, the depth of PEEK material increases as laser power, and the number of passes get high. Or it reduces as laser speed and frequency get low. When the number of passes increases, more heat is added to the polymer's profile. The maximum depth 2000 μm was at 25w, 20mm/s, 55 kHz, 7 per pass.

3. The number of passes modified the width of the top surface. When the number of passes seemed to be high, there was more heat in contact with the surface, and after 30W of power, a small width duty at a higher intensity caused MRR to happen more quickly than at other low levels. Small top width at a laser power of 25 W, laser speed of 40 mm/s, laser frequency of 55 kHz, and three passes, the minimum top kerf width was 305.56 m.

4. Both High passes and laser power reduces kerf taper. Due to increased heat energy and material removal rate, additional passes increase the depth and top width, and cases increase in focal length. At 40W, 30mm/s, 60 kHz, and five passes, the minimum angle is 2.8906^{o}.

5. It is important to use a set of laser conditions that offer high-quality kerf feature values to enhance the quality of laser micro-cutting processes. With moderate laser power, moderate laser passes, and many velocities offer a good cut.

NOMENCLATURE

f	ıser Frequency
k	e Number of Variables
N	presents The Experiments Number
P. N	sses Number
V	tting Speed
x	ɔut Parameter
α	ial Point Constant
β	nstants to The Regression Equation
ε	sidual Error
γ	e Response (Output)
Adj MS	Mean square
Adj SS	The Sum of Squares
BBD	Box Behnken Design
CAD	Computer-Aided Design
CCD	Central Composite Design
DF	Degree of freedom
DOE	Design Of Experiments.
HAZ	Heat Affected Zone
MID	Molded Interconnection Devices
MRR	Material Removal Rate
ND: YAG	Neodymium-Doped Yttrium Aluminum Garnet
PEEK	Polyether Ether Ketone
PMMA	Poly Methyl Meth Acrylic
RSM	Response Surface Methodology
SSE	Sum of Squares of Error
SST	Total Sum Square

REFERENCES

Bachy, B., and Franke, J., 2015. Experimental investigation and optimization for the effective parameters in the laser direct structuring process. *Journal of Laser Micro Nanoengineering*, *10*(2), P.202. doi:10.2961/jlmn.2015.02.0018.

Bachy, B., 2017. *Experimental investigation, Modeling, Simulation and Optimization of Molded Interconnect Devices (MID) Based on Laser Direct Structuring (LDS)*. Friedrich-Alexander-Universität Erlangen-Nürnberg (FAU).

Baş, D., and Boyacı, I.H., 2007. Modeling and optimization I: Usability of response surface methodology. *Journal of food engineering*, *78*(3), pp. 836-845. doi:10.1016/j.jfoodeng.2005.11.024

Dixit, S. R., Das, S. R., and Dhupal, D., 2019. Parametric optimization of Nd:YAG laser micro grooving on aluminum oxide using integrated RSM-ANN-GA approach. *J. Ind. Eng. Int,* 5(2), pp. 333–349. doi:10.1007/s40092-018-0295-1.

Genna, S., Menna, E., Rubino, G., and Tagliaferri, V., 2020. Experimental investigation of industrial laser cutting: The effect of the material selection and the process parameters on the kerf quality. *Applied Sciences*, *10*(14), P.4956. doi:10.3390/app10144956.

Girdu, C.C., Gheorghe, C., Radulescu, C., and Cirtina, D., 2021. Influence of process parameters on cutting width in CO2 laser processing of hardox 400 steel. *Applied Sciences*, *11*(13), P.5998. doi:10.3390/app11135998.

Madić, M., Petrović, G., Petković, D., Antucheviciene, J., and Marinković, D., 2022. Application of a robust decision-making rule for comprehensive assessment of laser cutting conditions and performance. *Machines*, *10*(2), P. 153. doi:10.3390/machines10020153

Mishra, D.R., Dutt, G.G., Prakash, D., Bajaj, A., Sharma, A., Bisht, R., and Gupta, S., 2020. Optimization of kerf deviations in pulsed Nd: YAG laser cutting of hybrid composite laminate using GRA. *FME Transactions*, *48*(1), pp. 109-116. doi:10.5937/fmet2001109M.

Mushtaq, R.T., Wang, Y., Rehman, M., Khan, A.M., and Mia, M., 2020. State-of-the-art and trends in CO2 laser cutting of polymeric materials—a review. *Materials*, *13*(17), P.3839. doi:10.3390/ma13173839

Ninikas, K., Kechagias, J., and Salonitis, K., 2021. The impact of process parameters on surface roughness and dimensional accuracy during CO2 laser cutting of PMMA thin sheets. *Journal of Manufacturing and Materials Processing*, *5*(3), P.74. doi:10.3390/jmmp5030074.

Patel, A., and Bhavsar, S.N., 2021. Experimental investigation to optimize laser cutting process parameters for difficult to cut die alloy steel using response surface methodology. *Materials Today: Proceedings*, *43*, pp. 28-35. doi:10.1016/j.matpr.2020.11.201

Pramanik, D., Kuar, A.S., Sarkar, S., and Mitra, S., 2021. Optimisation of edge quality on stainless steel 316L using low power fibre laser beam machining. *Advances in Materials and Processing Technologies*, *7*(1), pp. 42-53. doi:10.1080/2374068X.2020.1745734

Rodrigues, G. C., Vorkov, V., and Duflou, J. R., 2018. Optimal laser beam configurations for laser cutting of metal sheets. *Procedia CIRP*, 74, pp. 714–718. doi: 10.1016/j.procir.2018.08.026.

Sen. A, Doloi. B., and Bhattacharyya. B, 2016. Fiber laser micro channeling of polymethyl methacrylate (PMMA). *Lasers Eng.*, 35(14), pp. 123–138

Son, S., and Lee, D., 2020. The effect of laser parameters on cutting metallic materials. *Materials*, *13*(20), p.4596. doi:10.3390/ma13204596.

Spena, P.R., 2017. CO2 laser cutting of hot stamping boron steel sheets. *Metals*, *7*(11), p.456. doi:10.3390/met7110456.

Tamilarasan, A., and Rajamani, D., 2017. Multi-response optimization of Nd: YAG laser cutting parameters of Ti-6Al-4V superalloy sheet. *Journal of Mechanical Science and Technology*, 31, pp.813-821. doi:10.1007/s12206-017-0133-1.

Teixidor Ezpeleta, D., Ciurana, Q.D., and Rodríguez González, C.Á., 2014. Dross formation and process parameters analysis of fibre laser cutting of stainless steel thin sheets. *International Journal of Advanced Manufacturing Technology*, 2014, vol. 71, p. 1611-1621. doi:10.1007/s00170-013-5599-0

Varsi, A.M., and Shaikh, A.H., 2019. Experimental and statistical study on kerf taper angle during CO2 laser cutting of thermoplastic material. *Journal of Laser Applications*, 31(3), p.032010. doi:10.2351/1.5087846

Wang, X., Huang, Y., Wang, X., Xu, B., Feng, J., and Shen, B., 2020. Experimental investigation and optimization of laser induced plasma micromachining using flowing water. *Optics & Laser Technology*, 126, P.106067. doi:10.1016/j.optlastec.2020.106067